Strain path changes in aluminum

Cite as: AIP Conference Proceedings **2113**, 160013 (2019); https://doi.org/10.1063/1.5112710
Published Online: 02 July 2019

G. Vincze, M. C. Butuc, F. Barlat, A. B. Lopes, and T. F. V. Silva

Strain Path Changes in Aluminum

G. Vincze[1, a)], M.C. Butuc[1, b)], F. Barlat[2, c)], A.B. Lopes[3, d)] and T.F.V. Silva[3, e)]

[1]*Center for Mechanical Technology and Automation, Department of Mechanical Engineering, University of Aveiro, Campus Universitário de Santiago, 3810-193, Portugal.*
[2]*Graduate Institute of Ferrous Technology, Pohang University of Science and Technology, Pohang, Gyeongbuk 790-784, South Korea*
[3]*CICECO – Aveiro Institute of Materials, Department of Materials and Ceramic Engineering, University of Aveiro, Campus Universitário de Santiago, 3810-193, Portugal*

[a)]Corresponding author: gvincze@ua.pt
[b)]cbutuc@ua.pt
[c)] f.barlat@postech.ac.kr
[d)]augusto@ua.pt
[e)]tiagofvs@ua.pt

Abstract. Sheet metal forming processes involve large plastic deformation and changes in strain path. In this work, a detailed analysis of a commercially pure aluminum sheet subjected to tension-tension sequences with pre-strain in the rolling direction (RD) and reloads along different directions is presented, taking into consideration the mechanical behavior and texture evolution. Two main hardening behavior tendencies are observed, depending whether the reloading direction occurs for an angle smaller or larger than 45º.

INTRODUCTION

In a world where the concern with the environment is increasing, the choice of aluminum alloys for application in diverse industries such as packaging, automotive or aerospace is an intelligent option. The advantage of aluminum over others materials like steels or composites, resides on its lower density and the facility of recycle. Independently of the material selected for one application, the strong competitiveness imposes high-quality product with low cost. One way to attain this goal is the reduction of scrap during processes, which can be achieved by a deep understanding of material response to industrial forming operations.

Strain path changes is present in all the sheet metal forming processes. The knowledge of the origin of a particular effect is important in order to control the final shape of the product. Although many studies have been dedicated to this topic, due to a large number of strain path change combinations and existing materials, it is still an open research area. The material response to a single strain path change depends on its amplitude, which was very nicely characterized by Schmitt et al. (1985) [1] through the parameter α:

$$\alpha = \frac{d\varepsilon_p . d\varepsilon}{\|d\varepsilon_p\| \|d\varepsilon\|} \quad (1)$$

where dε and $d\varepsilon_p$ represent, the plastic strain tensors before and after the strain path change. The range of α is between 1 and -1, which correspond to monotonic and reverse loading, respectively, while 0 occurs for cross loading. Useful data regarding strain path change of aluminum alloys can be found in [2,3,4,5,6,7] where sequences like tension-shear,

Proceedings of the 22nd International ESAFORM Conference on Material Forming
AIP Conf. Proc. 2113, 160013-1–160013-6; https://doi.org/10.1063/1.5112710
Published by AIP Publishing. 978-0-7354-1847-9/$30.00

tension-compression, rolling-tension, forward-reverse simple shear, tension-tension have been investigated. In this work, we focus on the mechanical behavior of material loaded in tension-tension with special attention on crystallographic texture evolution.

MATERIAL AND EXPERIMENTAL DETAILS

The material studied in this work is a commercially pure AA1050 sheet sample, 3 mm thick, received in the H24 condition. The chemical composition is presented in table 1.

TABLE 1. Chemical composition of AA1050

Si	Fe	Cu	Mn	Mg	Cr	Ni	Zn	Ti	Ga	V
0.089	0.28	0.002	0.001	0.001	0.001	0.003	0.005	0.011	0.016	0.007

The behavior of this AA1050-H24 sheet sample was evaluated for non-linear deformation paths consisting of two uniaxial tension segments. The complete range of strain path changes from monotonic to pseudo-reverse loading was described by a rotation of the reloading axis with respect to the prestrain axis.

Large dog-bone samples were cut from as received material sheet and then subjected to RD uniaxial tension test with a pre-strain of 13.3%. From these pre-deformed specimens, small samples were cut at every 15º from the RD up to 90º and reloaded in uniaxial tension. For both size specimens, the cross-head velocity was adjusted to obtain an initial strain rate of 10^{-3}/s. The strain measurement in two directions was made by a videoextensometer Messphysik ME-46. All tests were performed at room temperature.

The crystallographic orientation (texture) was measured in the as received material and after pre-strain using a HR-FE SEM Hitachi SU70 equipment operating at 25 kV and equipped with a Quantax Cryst Align EBSD system from Bruker. The effect of texture was accounted by the VPSC polycrystal model developed by Lebenson and Tomé [8].

RESULTS AND DISCUSION

Microstructural characterization

The as received material presents an average grain size of about 40 μm, showing some variation between 20-80 μm for different zones as it can be observed in Fig. 1.

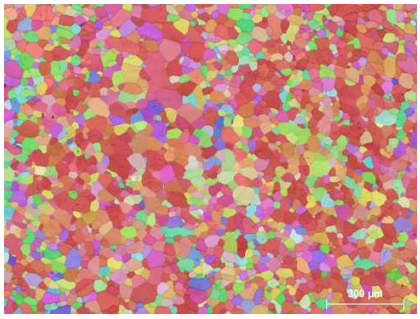

FIGURE 1. EBSD of initial material.

Regarding the grain orientations, the Cube texture is present in the as received material (Fig. 2a) and new components namely Copper, S and Brass (Fig. 2b) are formed during the pre-strain.

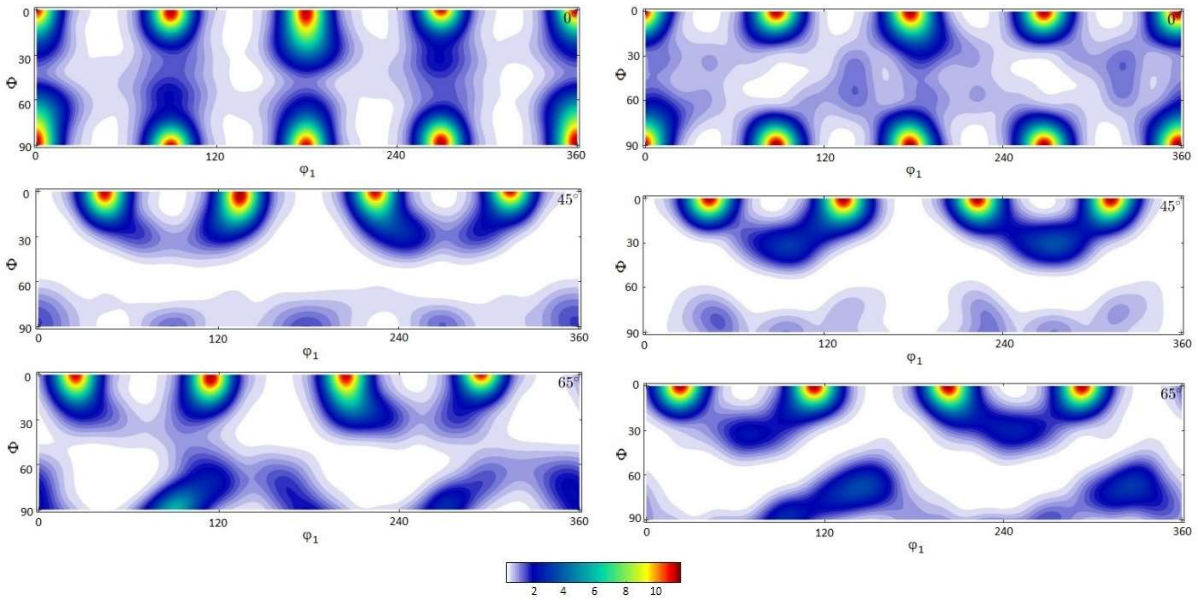

a) b)

FIGURE 2. ODF of the initial material (a) and after 13.3% prestrain (b).

Mechanical behavior

The mechanical behavior of as received and pre-strained material is presented in Fig. 3 a) and b), respectively, for stress-strain curves and complemented by the information from Figs. 4 and 5, where the values of Lankford coefficient, hardening coefficient, ultimate tensile strength and yield stress are presented for each loading orientation. The material presents an initial planar anisotropy. This can be observed in Fig. 3 a), by the variation of the stress-strain curves with the cut angle of the specimens, showing as an upper bound the curves corresponding to 0º and as a lower bound the curve corresponding to 90º. The hardening coefficient is almost constant for all the loading directions. A very small increase, less then 3% is observed for 30º, 45º and 60º. After reloading, a very small fluctuation (1.5 %) is observed for the tests corresponding to 45º-90º from RD (Fig. 4).

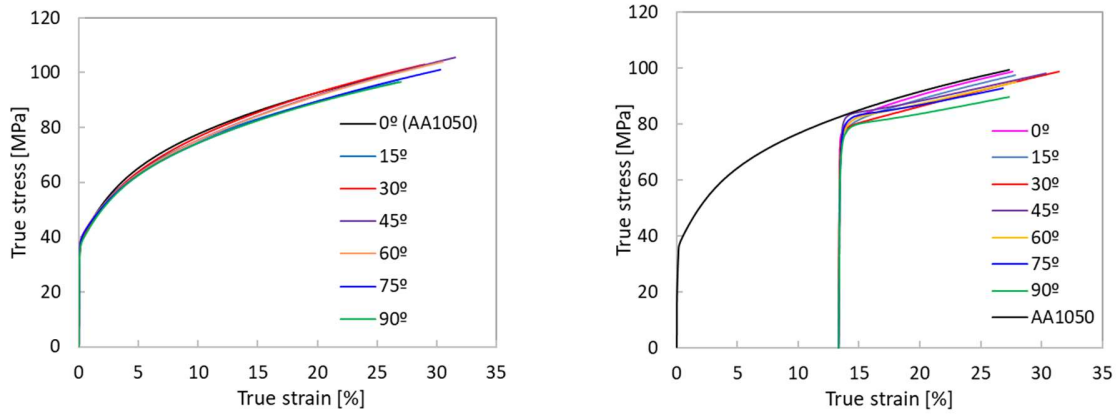

a) b)

FIGURE 3. True stress-true strain curves of as-received (a) and reloaded (b) material after 13.3% pre-strain.

The Lankford coefficient or r-value of as received material presents a minimum for 45º (very close of the value corresponding to 30º) and a maximum for 90º. After prestrain, it seems that r increases for all the angles orientation except for 30º, which shows a minimum. But the case of 30º should be studied in future since only data from one test

was available (Fig. 4). This effect on r-value is presumably due to the new texture components developed during the pre-strain. The yield stress of the as-received material shows a very small variation. After prestrain, the yield stress shows values similar to the UTS of the as-received material and some fluctuations of this parameter depending on the reloading direction are observed. Moreover, starting with 45º, the presence of rounded yield stress is observed (Fig. 6). This behavior is usually typical for reverse loading as shown in the literature.

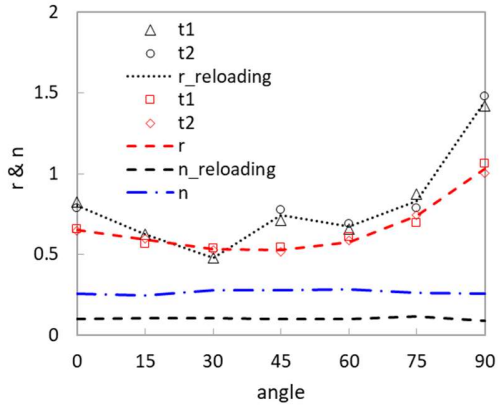

FIGURE 4. Lankford and hardening coefficients of as received and reloaded material for each loading direction.

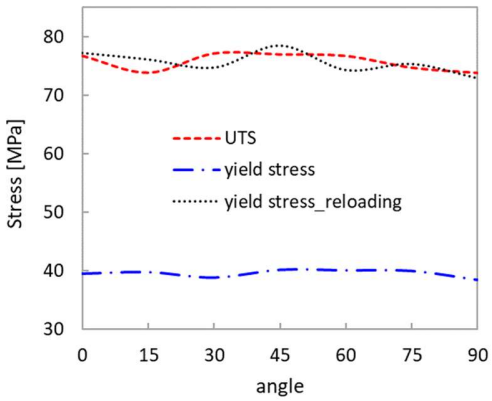

FIGURE 5. Variation of yield stress and ultimate tensile stress with the loading direction.

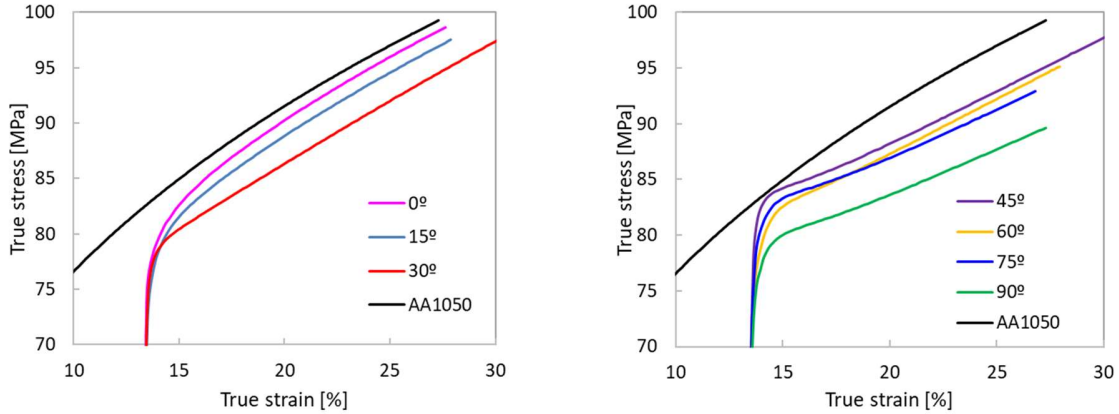

FIGURE 6. True stress-true strain curves of reloading, showing two type of responses.

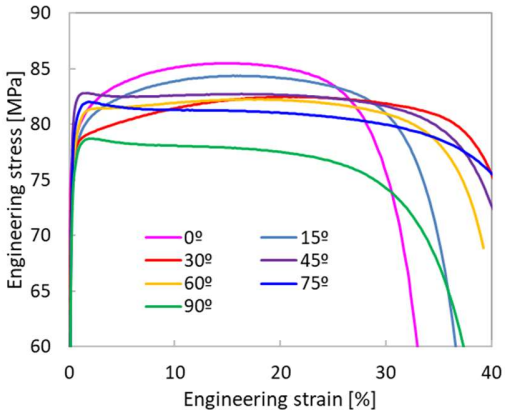

FIGURE 7. Engineering stress-engineering strain curves of reloading. Plastic instability occurs for 45º, 60º, 75º and 90º

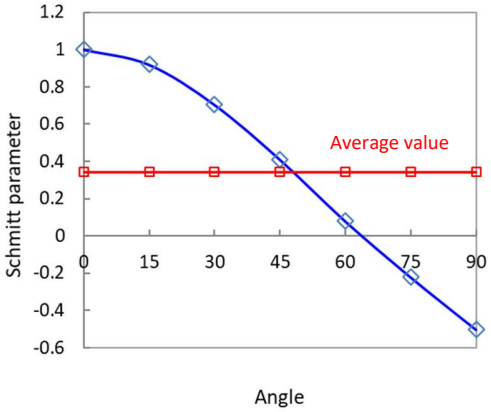

FIGURE 8. Variation of the Schmitt parameter of AA1050-H24 for the present loading conditions.

Figure 6 shows the true stress-true strain curves after reloading, divided into two patterns as follows: i) one corresponding to 0º, 15º and 30º, showing a behavior similar to pre-strain loading (shown for comparison purpose and labeled "AA1050"), where the curves are almost parallel; and ii) the second corresponding to 45º, 60º, 75º and 90º, showing a rounded yielding, some transient hardening and different strain hardening behavior compared to the reference curve. In fact, these two patterns, can be associated to the hardening and softening behavior according to the engineering stress-strain curves presented in Fig. 7. Fig. 8 shows the variation of Schmitt parameter for the present loading conditions, namely tension followed by tension. It can be observed that the change in the material response occurs for an angle at which α and the average value of α intersect.

The normalized stress with respect to the reference curve is plotted as a function of the strain for each reloading direction in Fig 9. The trend of these curves confirms the two regions described before. For 30º, a small variation from 0º and 15º is visible, but the real transition is completely activated at 45º.

In order to account for the contribution of texture for the observed behavior, the average VPSC Taylor factor <M> was calculated using the VPSC code starting from the experimental texture obtained after prestrain (Fig. 2 b). The results are presented in Fig. 10. The calculation of <M> captures the decreasing stress level from 0º to 90º, but attributes the same trend to 15º, 45º and 60º, which does not correspond to the experimental results. The same happens with the set of 30º, 75º and 90º. Consequently, it is concluded that a complementary analysis that takes the microstructure evolution into account is necessary in order to explain the material response for this strain path change. This will be the topic for future research.

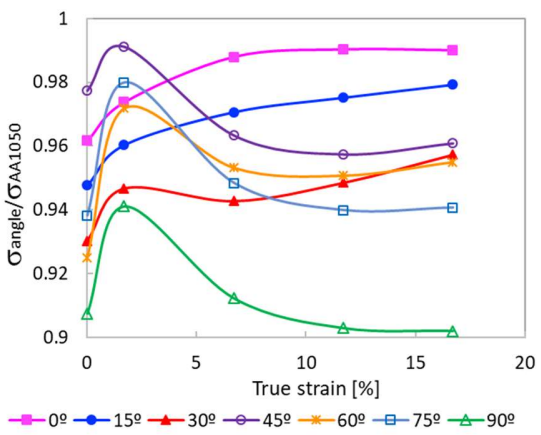

FIGURE 9. Normalized flow stress of reloading tests for different amount of strain.

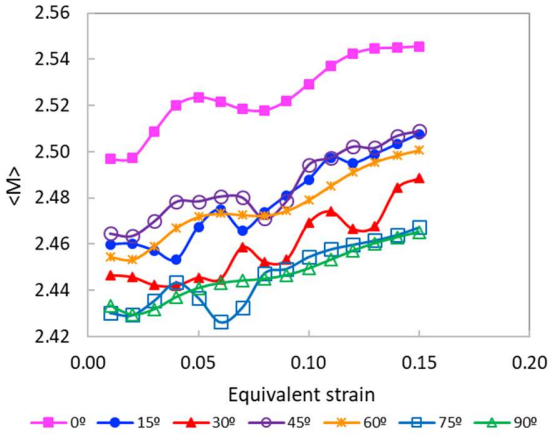

FIGURE 10. The average Taylor factor (<M>) extracted with VPSC model from the experimental crystallographic textures after prestrain.

CONCLUSIONS

The strain path change behavior of commercially pure aluminum sheet in the H24 state was investigated using sequences of two uniaxial tension segments. The material exhibits a strain hardening response for reloading at 0º, 15º and 30º and softening for 45º, 60º, 75º and 90º. Using the Euler angles as input of the measured texture after prestrain, the VPSC model was used to calculate the evolution of the VPSC Taylor factor with the equivalent strain for each reloading direction. The results show that the texture is not the main source of material response and additional investigation based on microstructure evolution is required.

ACKNOWLEDGMENTS

The authors acknowledge support from the Operational Program for Competitiveness and Internationalization, in its FEDER/FNR component and the Portuguese Foundation of Science and Technology (FCT), in its State Budget component (OE) through projects POCI-01-0145-FEDER-032362, UID/EMS/00481/2013 and CENTRO-01-0145-

FEDER-022083. The authors would like to thank to Dr. Carlos Tome (LANL) for providing the visco-plastic self-consistent polycrystal software.

REFERENCES

1. J.H. Schmitt, E. Aernould, B. Baudelet, Mater. Sci. Eng. **75**, pp. 13–20, (1985).
2. F. Barlat, J.M. Ferreira Duarte, J.J. Gracio, A.B. Lopes, E.F. Rauch, Int. J. Plast. **19**, pp. 1215–1244, (2003).
3. A.B. Lopes, F. Barlat, J.J. Gracio, J.F. Ferreira Duarte, E.F. Rauch, Int. J. Plast. **19**, pp. 1–22, (2003).
4. G. Vincze, E.F. Rauch, J.J. Gracio, F. Barlat, A.B. Lopes, Acta Mater. **53**, pp. 1005, (2005).
5. T. Mánik, B. Holmedal, O.S. Hopperstad, Int. J. Plast. **69**, pp. 1–20, (2015).
6. J. Qin, B. Holmedal and O. S. Hopperstad, Int. J. Plast. **101**, pp. 156–169, (2018).
7. M.C. Butuc, F. Barlat, J. Gracio, G. Vincze, Key Eng. Mater., **554-557**, pp. 127-138, (2013)
8. R.A. Lebensohn, and C.N. Tome´, Acta Metall. Mater. **41**, pp. 2611–2624, (1993).